Shifting carbonate burial between oceanic and continental crust across Earth history

Jon M. Husson and Shanan E. Peters

2026

Original citation:
Husson, J. M., & Peters, S. E. (2026). Shifting carbonate burial between oceanic and continental crust across Earth history. *Earth and Planetary Science Letters*, 677, 119810. https://doi.org/10.1016/j.epsl.2025.119810

Earth Planet. Sci. Lett. 677 (2026) 119810

Contents lists available at ScienceDirect

Earth and Planetary Science Letters

journal homepage: www.elsevier.com/locate/epsl

Shifting carbonate burial between oceanic and continental crust across Earth history

Jon M. Husson [a,*], Shanan E. Peters [b]

[a] School of Earth and Ocean Sciences, University of Victoria, Victoria, V8W 2Y2, BC, Canada
[b] Department of Geoscience, University of Wisconsin – Madison, 1215 W. Dayton Street, Madison, 53706, WI, USA

ARTICLE INFO

Dr Tristan Horner

Keywords:
Proterozoic-Phanerozoic transition
Global $CaCO_3$ cycle
Oceanic vs. continental sediment burial
Carbon recycling

ABSTRACT

Chemical weathering fluxes determine carbonate burial rates on geologic timescales, but the locus of carbonate burial is sensitive to tectonic and biologic boundary conditions that have changed across Earth history. Depositional setting is important because sediments on oceanic crust are readily recycled on the timescale of seafloor subduction, whereas sediments on continental crust can be sequestered over much longer durations. Here we present records of carbonate abundance in continental sediments for the past 3600 million years based on the North American components of the Macrostrat geologic column database and globally-distributed geological map units. Whether carbonate abundance is measured in absolute (area, volume) or in relative terms (carbonate normalized by total sediment), secular patterns emerge. In the Precambrian, carbonate abundance in continental crust is generally low. In the Phanerozoic, it climbs abruptly to a Paleozoic maximum and then declines towards the present. Decrease in shelf carbonate abundance across the Phanerozoic has been previously documented, driven in part by evolving paleogeography and the early Mesozoic evolution of pelagic calcifiers, which helped to shift carbonate burial from continental to oceanic crust. A Precambrian low in continental carbonate has received less attention. Here we propose that carbonate burial during much of the Precambrian was dominated by accumulation on (or within) oceanic crust and then shifted to continental crust in the early Paleozoic. Carbonate burial fluxes calibrated from the surviving rock record are an order of magnitude larger in the early Paleozoic than they appear to have been in the Proterozoic, with a step-wise increase occurring during the Ediacaran-Cambrian transition. This observation implies a large and relatively abrupt shift in the principal locus of $CaCO_3$ burial, from short-lived oceanic crust during much of the Proterozoic to longer-surviving continental crust in the early Paleozoic. Oceanic crust became, once again, a significant locus for carbonate accumulation during the Mesozoic and Cenozoic. The Paleozoic accommodation of most of the global carbon burial flux on the continents has many implications, including for secular changes in carbon cycling rates and the sensitivity of the surface environment to CO_2 injections.

1. Introduction

Across Earth history, changes in atmospheric CO_2 are determined by the difference between carbon input to the surface (including mantle degassing, metamorphism of carbon-bearing rocks, and weathering of organic carbon) and carbon burial in sediments (carbonate minerals and organic carbon, Hayes and Waldbauer, 2006). On timescales $>10^3$ years, the global flux of alkalinity produced by chemical weathering is balanced by the burial of carbonate minerals (Broecker and Peng, 1987). On geologic timescales ($\sim 10^5$ years and longer), the temperature dependence of chemical weathering rates acts as a negative feedback for global climate, thereby stabilizing surface temperatures (Walker et al., 1981).

Despite these controls operating throughout Earth history, the properties of carbonate sediment and its locus of deposition have changed considerably. A better understanding of this aspect is important because where $CaCO_3$ sediments are formed helps determine their long-term stability. Carbonates deposited on continental crust can survive for $>10^9$ years, whereas carbonates deposited on oceanic crust enter subduction zones on much shorter timescales, where they can be recycled in volcanic arcs (Edmond and Huh, 2003; Johnston et al., 2011). Although the decarbonation efficiency of subducted sediments varies, recent reviews suggest that much of the down-going carbon is volatilized and reintroduced to the surface environment (Plank and Manning, 2019; Arzilli et al., 2023). The locus of carbonate burial is, therefore, central to

* Corresponding author.
E-mail address: jhusson@uvic.ca (J.M. Husson).

https://doi.org/10.1016/j.epsl.2025.119810
Received 28 August 2025; Received in revised form 20 November 2025; Accepted 23 December 2025
Available online 5 January 2026

determining potential carbon recycling rates and hence carbon fluxes to the surface environment. Furthermore, because $CaCO_3$ sediment in contact with seawater buffers the global ocean against transient acidification (Zeebe and Westbroek, 2003), the surface distribution of $CaCO_3$ affects the sensitivity of the Earth system to CO_2-associated environmental perturbations.

Broad descriptions of carbonate sedimentation often divide Earth history into three phases: the Paleozoic, the Mesozoic-Cenozoic, and the Precambrian. Shallow-water, cratonic deposits that include metazoan biomineralizers are dominant in the Paleozoic Era (Wilkinson and Walker, 1989). Deep ocean basins became a more prominent locus of carbonate burial in the Mesozoic, owing to a poleward shift of the continents (Walker et al., 2002), a reduction in flooded continental area, and the evolution of pelagic calcifiers (Boss and Wilkinson, 1991; Bown et al., 2004; Ridgwell, 2005; Milliman and Droxler, 1996). Most of the Precambrian lacked eukaryote producers of $CaCO_3$, and its carbonate record is dominated by inorganic and microbial precipitation, including crystal fans, isopachous cements and microdigitate stromatolites in the Archean through Mesoproterozoic, and carbonate muds and trap-and-bind stromatolites in the Neoproterozoic Era (Grotzinger and James, 2000).

The hypothesis that benthic precipitation (occurring on or within the seafloor) was more important during much of the Precambrian is also supported by theoretical models of the $CaCO_3$ cycle. These models predict higher bottom water $CaCO_3$ oversaturation in the Precambrian vs. the Phanerozoic, based on the dominance of inorganic carbonate precipitation (Zeebe and Westbroek, 2003), low levels of O_2 and weak gradients in $CaCO_3$ saturation state (Higgins et al., 2009), and high levels of DIC (Higgins et al., 2009; Bergmann et al., 2013). Given that the solubility of $CaCO_3$ increases as temperature decreases and pressure increases, if bottom waters are oversaturated, then surface waters likely will be too. In the Precambrian, precipitation in the surface ocean could have been inorganic or facilitated by microbial activity, such as photosynthesis by surface-dwelling cyanobacteria (Thompson et al., 1997; Dittrich et al., 2004), which could have been present in both near- and off-shore settings (Buitenhuis et al., 2012). Higher bottom water $CaCO_3$ oversaturation would have also facilitated the preservation of any surface-produced carbonate sediment transported to deeper waters.

Given the possibility for both expanded bottom water oversaturation and export of surface produced $CaCO_3$, could the Precambrian have been similar to the Mesozoic-Cenozoic in terms of the importance of oceanic basins for carbonate deposition? It is commonly assumed that the Precambrian sedimentary $CaCO_3$ cycle was akin to the Paleozoic in terms of the locus of carbonate burial and the importance of shallow-water deposits (e.g., Ridgwell, 2005), although this notion has been challenged. Values of $\delta^{88/86}$Sr have been used to argue for the importance of carbonate burial on (or within) the Precambrian deep ocean seafloor (Wang et al., 2023), because $\delta^{88/86}$Sr values of preserved Precambrian carbonates are too high to achieve mass balance with assumed Sr inputs, thus implying a now-missing carbonate sink with low $\delta^{88/86}$Sr. Diagenesis remains a challenge in interpreting this record, however, as early alteration appears to shift carbonate $\delta^{88/86}$Sr to higher values (Kalderon-Asael et al., 2025). Furthermore, a similar approach that uses calcium isotopes does not provide similar evidence for a missing carbonate sink (Blättler and Higgins, 2017), as the average δ^{44}Ca value of Precambrian carbonates matches the isotopic value of the long-term value of Ca input to the oceans.

These proxy approaches are useful because direct evidence regarding Precambrian deep ocean $CaCO_3$ burial is limited due to the absence of any intact oceanic crust older than ~200 Ma. There are Paleozoic and Precambrian volcanic-sedimentary assemblages interpreted as ophiolites (Furnes et al., 2014, 2015), but they are typically tectonically dismembered and metamorphosed, which makes reconstructing their original sedimentary components challenging. Furthermore, most preserved Proterozoic ophiolites (77%) contain oceanic crust interpreted to have formed in backarc/forearc settings (Furnes et al., 2015), meaning this record is unlikely to represent average Precambrian oceanic crust.

To provide constraints on the locus of carbonate burial over Earth history, we present records of carbonate abundance in continental sedimentary rocks over the past 3600 million years (Myr.), based on the North American component of the Macrostrat database (Peters et al., 2018) and geologic maps covering Australia (Raymond et al., 2012), the Arctic (Harrison et al., 2011) and Europe (Asch, 2003), and portions of North America. For the past 125 Myr., the continental North American record is compared to a collection of deep sea cores also in Macrostrat (Fraass et al., 2015; Peters et al., 2018).

Today, shallow-water and carbonate-rich sediments are most abundant at low latitudes, owing in part to the temperature dependence on $CaCO_3$ solubility (Morse, 2005). Because this dependence has a mineral chemistry control, preferential deposition of carbonate at low-latitudes should be detectable throughout Earth history. Therefore, paleogeography is important to consider when evaluating carbonate accumulation on continental blocks. Here, the paleolatitudes of ancestral North America (Laurentia from Swanson-Hysell, 2021; Torsvik and Cocks, 2017) and Australia (western Australia from Merdith et al., 2017; Torsvik and Cocks, 2017) are reconstructed from paleogeographic rotation models and then compared to carbonate abundance data from these same regions.

2. Datasets and methods

Stratigraphic data from North America are derived from Macrostrat (https://macrostrat.org), currently characterized by 949 composited columns that synthesize both surface and subsurface rock units. A total of 24,141 lithologically and chronostratigraphically defined rock units are contained within these columns, 21,784 of which contain sediments or metasediments (Peters et al., 2018). Each sedimentary unit is assigned a variety of physical attributes, including thickness, lithology, and a modeled age estimate derived from contact relationships and correlations to chronostratigraphic time intervals (Peters et al., 2018). These data allow for the amount and spatial distribution of specific rock lithologies in North America to be estimated for any given geologic age (Fig. 1A).

To augment North American columns, geologic maps that cover portions of North America (at scales from 1:50,000 to 1:2,000,000) are also analyzed, including the conterminous United States (Horton et al., 2017, see Supplementary Excel file for the full list of map resources used). Sedimentary map units are selected for analysis if they have age estimates (via assignment to geologic time intervals) and text descriptions detailed enough to allow for carbonate vs. non-carbonate sedimentary lithologies to be parsed (Fig. 1B, n = 6056). Table 1 describes the number of such sedimentary and carbonate units from this map, with the "carbonate" category including both pure carbonate and mixed carbonate-siliciclastic units. Table 1 also shows the percentage of units assigned to different interval types to give a sense of age resolution (e.g., 55.8% of Phanerozoic units are assigned to an Epoch, etc.).

To expand the geographic coverage beyond North America, geological maps of Australia (Fig. 1C), the Arctic (Fig. 1D) and Europe (Fig. 1E) are also analyzed. The Australian map (1:1,000,000 scale, Raymond et al., 2012) consists of 2447 sedimentary units (Table 1). The Arctic geologic map (1:5,000,000 scale, Harrison et al., 2011) covers all regions north of 60°N latitude (Fig. 1D), and thus has significant geographic overlap with the map of Europe (1:5,000,000 scale, Asch, 2003). A combined map was therefore created, with the European map clipped north of 60°N (Fig. 1E).

Geographic overlap also exists between the Arctic-Europe map and the North American datasets. Thus, Arctic units that intersect Laurentia (grey in Fig. 1A and B) were excluded, meaning that the analyzed Arctic-Europe map consisted of 2561 sedimentary units (Table 1). Complementarily, for North American Macrostrat, columns whose centroid

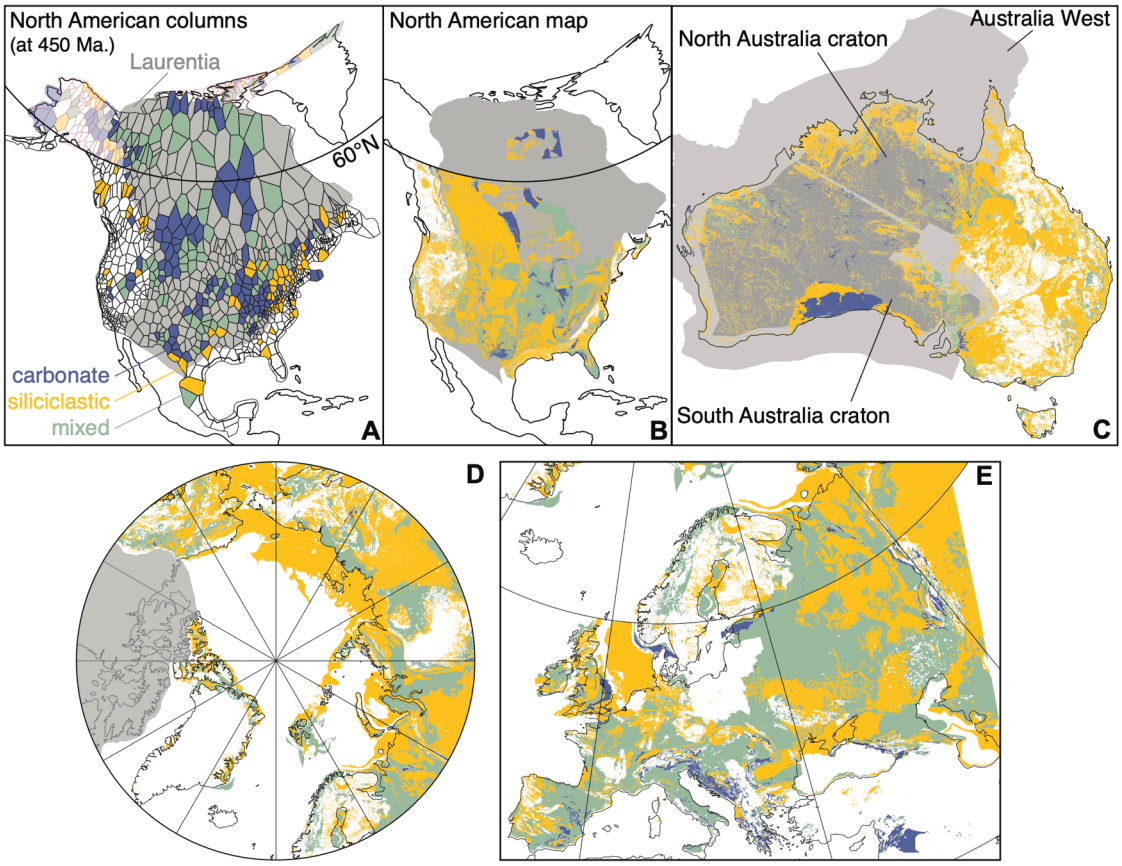

Fig. 1. Geologic syntheses analyzed in this paper. (A) Macrostrat database for North America (Peters et al., 2018), with columns highlighted that have sediment 450 Ma. in age, color-coded as all carbonate (blue), siliciclastic (yellow) or mixed carbonate-siliciclastic (green). Also shown is Laurentia (grey) used in paleogeographic reconstructions (Swanson-Hysell, 2021). Macrostrat columns that are located north of 60°N and outside of Laurentia are outlined in red. (B) Composite geologic map that covers portions of North America at a variety of scales (1:50K to 1:2M). (C) 1:1M scale compilation geologic map of Australia (Raymond et al., 2012), shown with the geometries used for Proterozoic paleogeographic reconstructions ("South Australia Craton" and "North Australia Craton" from Merdith et al., 2017) and Phanerozoic paleogeographic reconstructions ("Australia West" from Torsvik and Cocks, 2017). (D) 1:5M compilation maps of the Arctic (north of 60°N) from Harrison et al., 2011) and (E) Europe (Asch, 2003).

is north of 60°N were excluded (red outlines in Fig. 1A), unless they are located on Laurentia. The total number of North American columns in the final analyzed subset is 820 (black outlines in Fig. 1A) and contain 20,022 sedimentary units (Table 1). The geographic footprints of the North American, Arctic and European datasets examined here do not overlap with one another (Fig. 1A, B, D and E). Together, the datasets from geologic maps and Macrostrat cover ~40% of Earth's continental area.

3. Results

3.1. Absolute records of carbonate and sediment abundance

Time series of carbonate and total sedimentary abundance are tabulated in 1 Myr. increments, from 3600 Ma. to 0 Ma. For each age, the areas of all Macrostrat columns that contain units with any sediments/metasediments and any carbonate/metacarbonate are respectively summed; the two resulting time series are shown in Fig. 2A. We estimate uncertainty via 1000 bootstrap resamplings, in which the list of North American rock units (20,022) in columns (820) is sampled with replacement, and time series are calculated from this re-sampled list. Solid lines and shaded regions in Fig. 2A represent the median and the middle 68% of these 1000 bootstrapped time series, respectively (akin to the mean ±1 standard deviation, if the distribution is normal).

Surviving sedimentary rock area generally decreases with increasing geologic age, but these net decreases occur in three rather narrow time windows: between 0 Ma. and 5 Ma., between 500 Ma. and 550 Ma., and a more prolonged transition between 2800 Ma. and 3100 Ma. In between these short intervals, there are no clear secular trends in surviving sedimentary rock area; instead, values oscillate around long-term averages, especially within the Phanerozoic and Proterozoic eons (Fig. 2A). North American carbonate area generally follows the overall sedimentary record, although there is age-dependent variability in how well the two time series are correlated (Spearman's ρ on first differences: 0.32 (Proterozoic), 0.75 (Paleozoic), 0.46 (Mesozoic-Cenozoic)). A striking difference between the two is that North American carbonate area increases with increasing age throughout the Phanerozoic, a finding similar to previous work (Walker et al., 2002).

Time series of sedimentary and carbonate rock area from the North American, Arctic-European and Australian geologic maps were calculated analogously to Fig. 2A. However, because of the large difference in the average duration of time bins assigned to Precambrian vs. Phanerozoic map units (538 – 842 vs. 34 – 59 Myr., Table 1), the area of each map unit is first normalized by the duration of its assigned age bin before being summed, in an effort to dampen the influence of map units with very long apparent durations. The North American map time series has similarities to North American columns, although the changes in area between 0 – 5 Ma. and 500 – 550 Ma. are much more dramatic in the former (Fig. 2B, note logarithmic y-axis). In contrast to North America, the Arctic-European sedimentary map data do show persistent decline with increasing age across the full 3600 Myr. time

Table 1
Summaries of the datasets analyzed in this paper. "Sedimentary" are units that have one (or more) sedimentary lithology in their text description, and "carbonate" are a subset that also have at least one described carbonate lithology. Sedimentary map units are grouped into one of three categories: Phanerozoic (Phnz), Precambrian (PrCm) or boundary crossers (Phnz-PrCm), which have a Precambrian bottom age and a Phanerozoic top age. For the map datasets, the percentage of sedimentary units in these three groups assigned to different interval categories are also listed. Age estimates for Macrostrat sedimentary units are derived from the age model described in Peters et al. (2018).

		Number of units			Interval types in age assignments (%)					
Dataset	Scale		Sedimentary	Carbonate	Age	Epoch	Period	Era	Eon	other
Geologic maps:										
North America	1:50K to 1:2M	Phnz	5000	2284	14.5	55.8	27.8	1.0		1.0
		PrCm	738	147			14.0	72.5	10.5	3.0
		Phnz-PrCm	318	69	0.5	13.5	24.4	47.6	3.8	10.2
Australia	1:1M	Phnz	1495	444	29.8	50.5	16.6	3.2		
		PrCm	921	303			51.0	41.9	7.1	
		Phnz-PrCm	31	13		29.0	22.6	48.4		
Europe-Arctic	1:5M	Phnz	2275	1277	3.6	52.2	40.9	2.9		0.3
		PrCm	225	105			46.7	42.4	8.2	2.7
		Phnz-PrCm	61	44		2.5	36.1	44.3	14.8	2.5
Macrostrat columns:										
North America		Phnz	18,837	8626						
		PrCm	1119	294						
		Phnz-PrCm	66	17						
deep sea		Phnz	12,568	4467						

series (Fig. 2C). This decline, approximately exponential at least between 0 and 1500 Ma. (red dashed line in Fig. 2C), is also potentially seen in the Australian map sedimentary time series, but less clearly (Fig. 2D).

3.2. Normalized records of carbonate abundance

To remove any secular changes in carbonate rock quantity that result from changes in total sedimentary rock quantity, we calculate normalized estimates of carbonate rock abundance for each studied region (Fig. 3). For North American columns, the number of carbonate-containing columns that intersect with a given age is divided by the total number of all sediment-containing columns (blue curve in Fig. 3A). A binned approach was also used, where total counts of carbonate and sedimentary units that intersect a geologic period (and era in the Archean) are used to calculate a "bin fraction carbonate" value (grey boxes in Fig. 3A). These bin values approximate long-term averages of the continuous time series, except for the Archean Eon, where the low number of units mean that the continuous fraction carbonate value can more easily deviate from an era value.

For the map datasets, the total duration-normalized area of carbonate-containing map units that intersect with a given age is divided by the total duration-normalized area of sediment-containing map units (Fig. 3B–D). For all of these time series, a value of 1 would indicate that all sedimentary rock units of that age contain at least some carbonate, and 0 would mean that none do. Envelopes around the fraction carbonate curves, and the heights of the grey boxes in Fig. 3A, represent the middle 68% of 1000 bootstrap iterations, and solid blue line represents the median (Fig. 3).

Time series of these relative measures of carbonate abundance differ substantially from the non-normalized quantities (Fig. 2). For North American columns in the Precambrian (Fig. 3A), fraction carbonate is lowest in the Archean (especially the bin values), and rises to an average value of 0.26 for the Proterozoic. Carbonate fraction rises sharply from the Ediacaran through the Cambrian, reaching a maximum value of 0.85. It remains high throughout the rest of the Paleozoic Era before dropping to 0.35 at its end. Fraction carbonate remains low for the Mesozoic Era (mean of 0.28), and continues to drop into the Cenozoic (mean = 0.13). The time series derived from the North American map (Fig. 3B) is similar, with high correlation between the two North American time series (ρ = 0.85).

The Arctic-European fraction carbonate record shares similarities with the North American records. It also has near-zero values throughout the Archean (~0.01), with a sharp increase across the Archean-Proterozoic boundary (Fig. 3C). Values steadily rise throughout the Proterozoic, from 0.26 at its beginning to 0.80 at its end. A maximum value for the time series is reached in the early Paleozoic (0.95), then declines and is low across much of the Mesozoic (average of 0.36 between 251 and 101 Ma.). A notable difference from North America is that fraction carbonate values are high between 100 and 10 Ma. (0.66), before declining to zero towards 0 Ma.

Like North America and Arctic-Europe, carbonate fraction values from Australia are lower in the Archean than in the Proterozoic, except for the Neoarchean Era (Fig. 3D). This exception is due to the Fortescue Group, which includes the carbonates of Tumbiana Formation that have been interpreted as lacustrine owing to abrupt vertical and lateral facies changes argued to indicate non-marine deposition (Coffey et al., 2013). If these potentially terrestrial sediments are excluded, Neoarchean fraction carbonate drops to 0.16 (dashed blue line in Fig. 3D). Like Arctic-Europe, fraction carbonate in Australia rises throughout the Proterozoic, from 0.19 at the beginning to 0.51 – 0.61 by the end (Fig. 3D). However, unlike North America and Arctic-Europe, fraction carbonate values do not decline from the early Paleozoic towards the modern. Aside from relatively brief spikes to high values between 510 – 485 Ma., 360 – 325 Ma. and 25 – 5 Ma., Phanerozoic values are low and comparable to the Proterozoic.

4. Discussion

4.1. Patterns of carbonate abundance across Earth history

One of the most striking features of North American sedimentary rock quantity, measured from Macrostrat columns, is the lack of persistent decline with increasing rock age (Fig. 2A). Decline is present – there are more Pleistocene sediments than Archean sediments. But net decline in area with increasing age occurs in discrete, relatively short time spans, mostly between 5 and 0 Ma. and 550 and 500 Ma, the latter of which coincides with the Proterozoic-Phanerozoic transition and

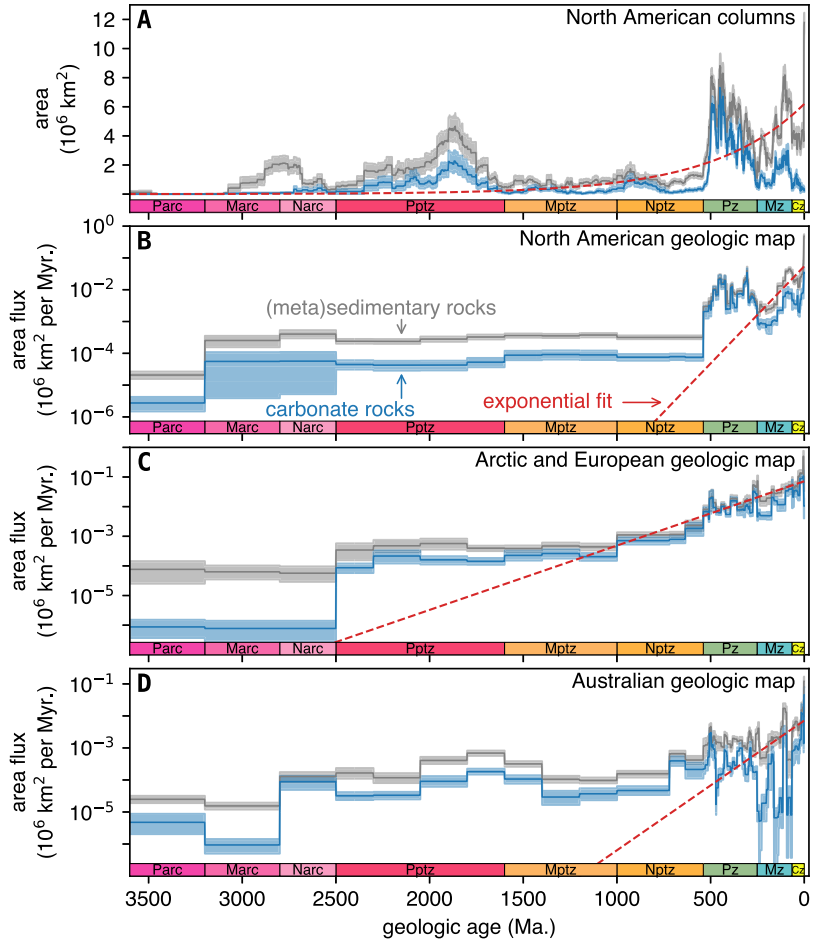

Fig. 2. Time series of rock area per million years for sedimentary (grey) and carbonate rocks (blue), measured from the North American Macrostrat columns (A) and geologic maps of North America (B), Europe and the Arctic (C) and Australia (D). Tabulations of sedimentary rocks include metasedimentary lithologies and carbonates include metacarbonates. Shaded regions cover 68% of the 1000 bootstrapped iterations of unit datasets from North American columns and North American, Australian, and Arctic-European maps, and solid lines are the median values. Red dashed lines are exponential fits to the sedimentary area time series (fit limits are 0 – 1000 Ma. for A and C, and are 0 – 250 Ma. for B and D). Note that the y-axis scale is logarithmic on subplots B, C and D. The abbreviations for eras labeled on the geologic time scales are: Paleoarchean (Parc), Mesoarchean (Marc), Neoarchean (Narc), Paleoproterozoic (Pptz), Mesoproterozoic (Mptz), Neoproterozoic (Nptz), Paleozoic (Pz), Mesozoic (Mz) and Cenozoic (Cz).

the Great Unconformity. These features of the North American sedimentary rock record have been documented and the implications for models of rock cycling and the evolution of Earth's surface environment have been discussed (Husson and Peters, 2017; Peters and Husson, 2017; Husson and Peters, 2018; Peters et al., 2022; Walton et al., 2023). Notably, the hypothesis that erosion and rock destruction is a dominant process that controls surviving continental sedimentary rock quantity is not well supported by these data. This is because a central prediction of all such models is a broadly exponential decline in surviving amount with increasing age (e.g., Gregor, 1970).

Approximately exponential decline is, however, observed when continental sedimentary rock area is measured from geological maps. This observation is found for Arctic-Europe (red dashed line in Fig. 2C) and for the Mesozoic-Cenozoic portions of the Australian and North American maps (red dashed line in Fig. 2B and D), and has been documented in other geologic map-derived datasets (Blatt and Jones, 1975; Peters and Husson, 2017). This feature of geologic map-based data is predominantly a signature of rock preservation: younger sedimentary rocks tend to bury older rocks, which contributes to their longevity yet removes them from inclusion in geologic map-based tabulations (Peters and Husson, 2017; Wilkinson and Consuegra, 2024). In this context, it is notable that sediment quantity data derived from Macrostrat columns on *oceanic* crust, which is continually subducted in an age-independent fashion (Rowley, 2002), does exhibit the exponential decrease with increasing age that is the prediction of standard rock cycling models (Peters et al., 2013; Peters and Husson, 2017; Peters et al., 2022).

Fraction carbonate time series (Fig. 3) allow changes in carbonate abundance to be assessed independently of any changes in overall sedimentary rock quantity. Proportions also facilitate comparisons of trends in carbonate abundance between different geographic regions and dataset types. The Arctic-European fraction carbonate time series (Fig. 3C) shares similarities with North America's record (Fig. 3A and B). Arctic-Europe map data are correlated with both the North American columns and map time series (ρ = 0.53 and 0.55, respectively), but the strength of correlation is weakened when calculated on first-differences (ρ = 0.23 and 0.18). More qualitatively, the similarities include maximum observed values in the early Paleozoic and a persistent decline from the Paleozoic towards the present. A chief difference is that Arctic-European values in the Proterozoic, although intermediate between Archean and Paleozoic values (akin to North America), show a rise from 2500 to 538.8 Ma. (absent in North America).

The Australian fraction carbonate record shows notable differences from both Arctic-Europe and North American records (Fig. 3D). Australian fraction carbonate generally rises between 3600 and 538.8 Ma., especially if the possibly lacustrine Fortescue Group (Coffey et al., 2013)

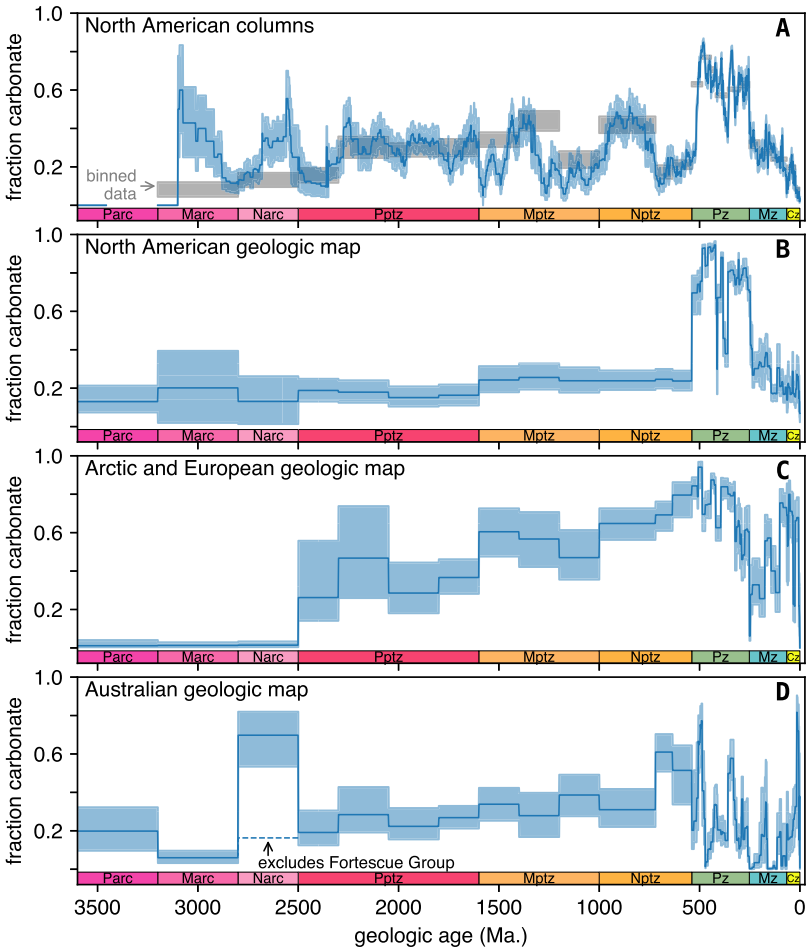

Fig. 3. Time series of fraction carbonate in Fig. 2 datasets: North American columns (A) and geologic maps of North America (B), Europe and the Arctic (C) and Australia (D). Blue shaded regions cover 68% of the 1000 bootstrapped iterations of each dataset; solid lines are medians. For North American columns (A), the grey rectangles cover 68% of the bootstrap iterations when the re-sampled unit list is first binned into geologic periods (eras in the Archean) before fraction carbonate (per bin) is calculated.

is excluded from the analysis (dashed blue line in Fig. 3D). This trend is similar to North America and Arctic-Europe. But unlike North America and Arctic-Europe, there is no Phanerozoic downward trend towards the present day, with Phanerozoic values instead oscillating around a low average value.

Importantly, the fraction carbonate time series do not support the hypothesis that preferential removal of more weatherable carbonates (e.g., Gaillardet et al., 1999) is a strong determinant of their abundance in the rock record. If this hypothesis were true, the data would show an overall decline in fraction carbonate relative to all sediment types with increasing sediment age. This trend is observed in the Precambrian portions of the time series, especially in Arctic-Europe and Australia (Fig. 3C and D). However, it is not observed in the Phanerozoic, where carbonate proportions decline towards the present (Fig. 3A–C) or show no clear trend (Fig. 3D), suggesting alternative controls on the relative abundance of carbonate, at least in the Phanerozoic (as has been argued previously, Walker et al., 2002).

4.2. Controls on carbonate abundance in the Phanerozoic

Within the Phanerozoic, the amount of $CaCO_3$ in continental sedimentary rocks declines towards the present (Figs. 2A and 3A–C). Previous work has recognized this trend, both as a North American (Berry and Wilkinson, 1994) and global (Ronov et al., 1980; Wilkinson and Walker, 1989; Walker et al., 2002) phenomenon. Changes in global paleogeography have been invoked as one cause, given latitudinal control on the accumulation of shallow-water carbonates, which today form predominantly within 30° of the equator (Lees, 1975). Given the poleward drift of continents throughout the Phanerozoic (Berry and Wilkinson, 1994; Walker et al., 2002), flooded continental shelves have generally become less amenable to carbonate accumulation over Phanerozoic time.

To assess this known geographic influence on carbonate accumulation, we compare the record of fraction carbonate calculated from Macrostrat columns located on Laurentia (7631 carbonate and 15,443 sedimentary units; Fig. 1A) to a paleogeographic rotation model for Laurentia that covers the last 1800 Myr. (Swanson-Hysell, 2021). Using *GPlates* (Müller et al., 2018), GIS shapefiles of paleogeographic reconstructions of Laurentia were created in 1 Myr. time steps in the Phanerozoic and in 10 Myr. time steps in the Protereozoic. For each reconstruction, the area of continent contained within 1° latitudinal bands was calculated. A similar procedure was followed for Australia, using a Neoproterozoic rotation model (1000 – 550 Ma.) for the "North Australia Craton" and "South Australia Craton" (Fig. 1C) from Merdith et al. (2017) and a Phanerozoic rotation model for "Australia West" (Fig. 1C) from Torsvik and Cocks (2017). Fraction carbonate time series were recalculated from map units that intersect these cratonic outlines (498 carbonate and 1377 sedimentary map units). Paleogeographic reconstructions were created in 1 Myr. time steps in the Phanerozoic and in 2 Myr. time steps between 1000 and 550 Ma. These calculations allow the fraction carbonate values (Figs. 4A and 5A) and latitudinal landmass distributions (Figs. 4B and 5B) for a given age to be compared directly (Fig. 6).

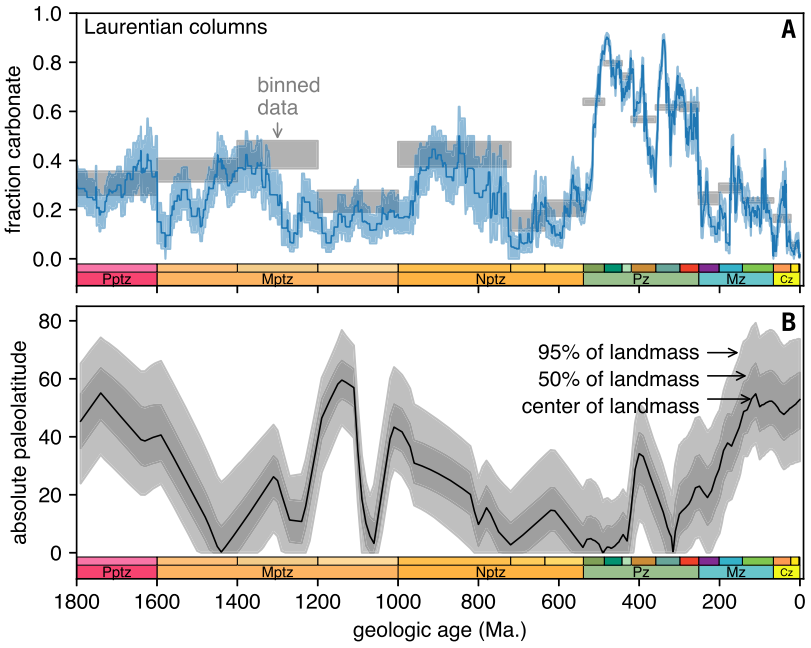

Fig. 4. (A) To allow direct comparisons to paleogeographic reconstructions, a time series of fraction carbonate is calculated using only Laurentian Macrostrat columns (see Fig. 1B). (B) This record is compared to Laurentia's latitudinal distribution through time, derived from a paleogeographic rotation model from Swanson-Hysell (2021). The black line and grey envelopes show the absolute paleolatitudinal extent of Laurentia.

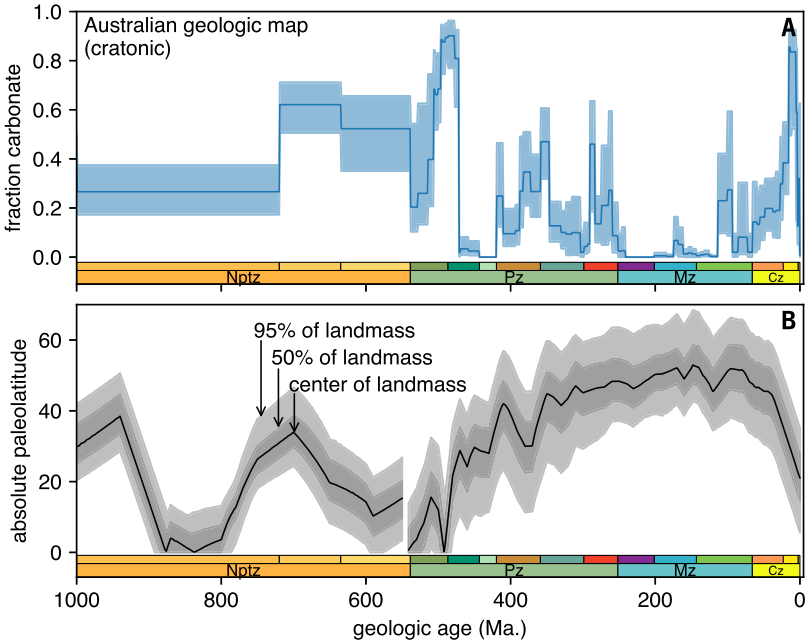

Fig. 5. (A) Similar to Fig. 4A, a time series of fraction carbonate is recalculated using only Australia map polygons that intersect the cratonic polygons in Fig. 1C. (B) Absolute paleolatitudinal extent of cratonic Australia through time, derived from paleogeographic rotation models for the Neoproterozoic Era (Merdith et al., 2017) and for the Phanerozoic Eon (Torsvik and Cocks, 2017).

In the Phanerozoic, the fraction carbonate record of Laurentia is anticorrelated with its absolute paleolatitude (Fig. 6A). During most of the Paleozoic, Laurentia was at low-latitudes (Fig. 4B). A northward drift began at ~310 Ma. and ended around ~110 Ma., and Laurentia has remained at mid- to high-latitudes since then (Fig. 4B). These Phanerozoic secular trends are mirrored in fraction carbonate, expressed as a negative correlation between fraction carbonate and the absolute paleolatitude of Laurentia's centroid ($\rho = -0.77$, Fig. 6A). A similar anticorrelation is also found in Phanerozoic data from Australia ($\rho = -0.61$, Fig. 6B), a time period when Australia was mostly poleward of the subtropics (Fig. 5B).

The paleolatitude of a continent's centroid is, however, not a perfect predictor of carbonate abundance. For example, in the Cambrian, when both Laurentia and Australia were entirely subtropical, fraction carbonate values range between 0.19 to 0.86 (Fig. 6A) and 0.21 to 0.90 (Fig. 6B), respectively. In the Cretaceous, when both Laurentia and Australia were mostly poleward of the subtropics, fraction carbonate values range between 0.01 – 0.41 (Fig. 6A) and 0.0 – 0.24 (Fig. 6B). Thus, low

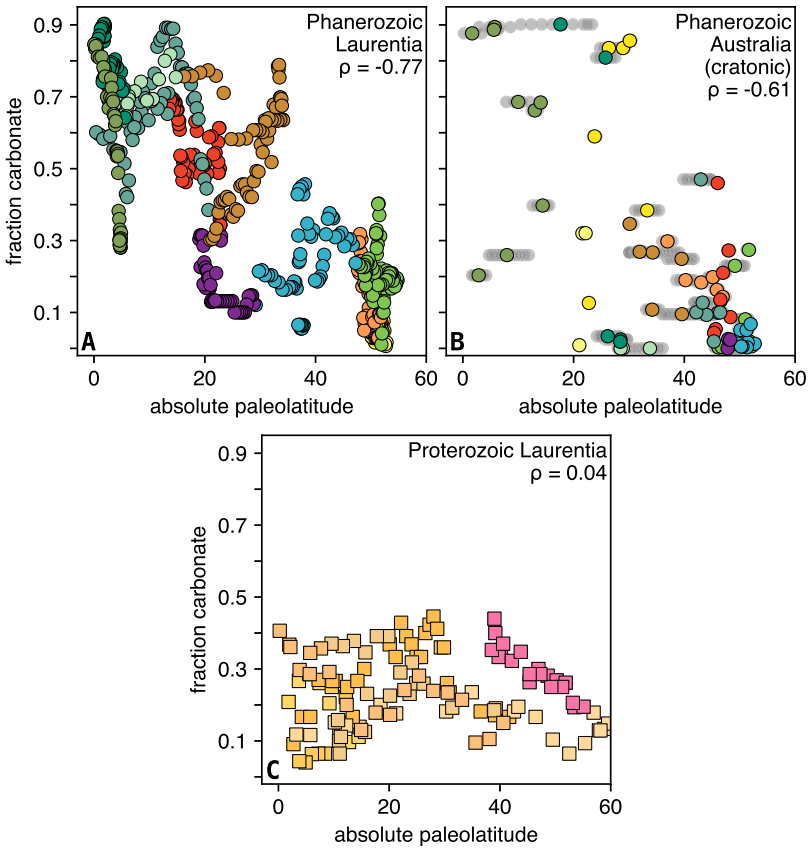

Fig. 6. Cross-plots show fraction carbonate vs. centroid absolute paleolatitude for Phanerozoic Laurentia (A), Phanerozoic cratonic Australia (B), and Proterozoic (1800 – 538.8 Ma.) Laurentia (C). These same data are plotted as time series in Figs. 4 and 5. Symbols (circles for Phanerozoic, squares for Proterozoic) are color-coded by their corresponding geologic period. Because the paleogeographic rotation model for Australia is more time resolved than its fraction carbonate record, the x-axis value for each color symbol is the average centroid paleolatitude for the given period-, epoch- or age-bin for which a unique fraction carbonate value is resolved (Fig. 5B). All the Australian paleogeographic data are also plotted in grey in the background.

fraction carbonate values are possible if a crustal block is either tropical or temperate-polar. However, the highest fraction carbonate values observed are generally found in time intervals when a continent is low latitude. This pattern suggests that low latitudes encourage carbonate accumulation in shallow water depocenters via high water temperatures and reduced $CaCO_3$ solubility (Morse, 2005), but does not guarantee it, as there are other controls on carbonate sedimentation – notably, siliciclastic sediment supply.

Another potential control on trends in Phanerozoic carbonate deposition is the evolution of pelagic calcifiers during the Triassic (Bown et al., 2004), which provided a metabolically-powered mechanism to shift $CaCO_3$ deposition from shallow continental settings to the deep sea (Wilkinson and Walker, 1989). Pelagic calcifiers made ocean crust an important locus for carbonate deposition during the past ~225 Myr., a transition that, perhaps not coincidentally, occurred in concert with a global poleward drift of continental shelves (Walker et al., 2002) and a decrease in continental flooding (Opdyke and Wilkinson, 1988; Kump and Arthur, 1997). A global shift to more prevalent deep sea carbonate sedimentation is another reason why North American fraction carbonate in the Mesozoic-Cenozoic is lower than it is in the Paleozoic (Fig. 3A and B), a pattern that is replicated in the Arctic-Europe time series (Fig. 3C). Australia does not clearly show this trend, likely because much of Australia was at high latitudes for the majority of the Paleozoic and Phanerozoic (from 450 Ma. onward, Fig. 5B).

Evidence for a reciprocal relationship between shallow and deep sea carbonate burial is evident over the last 125 Myr. when the North American column record is compared to data from 134 ocean drilling sites (Fraass et al., 2015; Peters et al., 2018). Fraction carbonate from sediments on oceanic crust shows a decrease from ~110 – 90 Ma., then an increase from ~90 – 60 Ma., and then a decrease from ~60 – 35 Ma (Fig. 7). The North American continental carbonate record shows the opposite pattern. Anticorrelation is, however, not apparent from ~35 Ma. onwards to the present day, during which time both records show a decrease. This shared decrease towards the present may reflect the global cooling trend observed for the latter Cenozoic Era, which could have decreased global carbonate burial through decreased carbonate weathering rates owing to declining temperatures (Gaillardet et al., 2019). Silicate weathering rates (and associated carbonate burial) may also have fallen, if volcanic outgassing rates also declined across the Cenozoic (e.g., Seton et al., 2009). Overall, however, the two time series are anticorrelated, with ρ = -0.37 calculated on a moving average with an 11 Myr. window (ρ = -0.74 if the datasets are restricted to between 125 and 35 Ma.). If the shelf is capable of trapping more carbonate because of, for example, changes in continental flooding and paleogeography (Opdyke and Wilkinson, 1988; Kump and Arthur, 1997), then the deep sea must accumulate less, provided that total carbonate burial remains broadly constant.

4.3. Controls on carbonate abundance in the Precambrian

Unlike in the Phanerozoic, paleolatitude does not show any relationship with fraction carbonate in Laurentia during the Proterozoic (Fig. 6C). Paleogeographic models predict that Laurentia covered a similar latitudinal range in both time intervals, with the absolute paleolatitude of its centroid ranging between 0 – 60° (1800 – 538.8 Ma.)

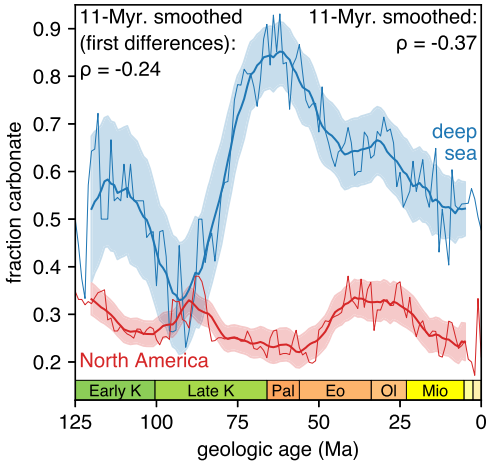

Fig. 7. A fraction carbonate time series calculated from North American Macrostrat (red) is compared to an analogous time series calculated from deep sea cores (blue) from the Atlantic, Pacific and Indian Oceans (Fraass et al., 2015; Peters et al., 2018). Uncertainty is estimated via bootstrapping (1000 iterations), as in Fig. 3. Lighter blue and red lines represent median value for fraction carbonate tabulated in 1 Myr. increments, and thicker lines are moving averages of these time series (11 Myr. window size). Shaded regions cover 68% of the 1000 bootstrap resamplings (also smoothed with a 11 Myr. window size).

and 0 – 55° (Phanerozoic). For ~25% of this Proterozoic time interval, all of Laurentia was within 30 degrees of the equator, but fraction carbonate never reached the highest values observed during the Paleozoic (Fig. 4A). This is true when also considering values calculated by geologic period (grey boxes in Figs. 3A and 4A), which will be less sensitive to errors in the estimated ages of sedimentary units. A lack of correlation in the Precambrian could indicate that paleogeography is less accurately reconstructed, or that there is significant error in Macrostrat's age model and/or its alignment with rotation models. Alternatively, it could reflect the fact that Laurentia was generally less accommodating for sediments and that it had much less marine flooded area, a situation that could result in the co-opting of limited low-latitude accommodation space by siliciclastic sediment.

When considered along with data from Arctic-Europe and Australia, low fraction carbonate values are globally widespread in Precambrian continental sediments (Fig. 3), especially for the Archean, Paleoproterozoic and Mesproterozoic. Overall, this suggests that oceanic crust, rather than continental crust, was a predominate locus of marine carbonate burial for much of the Precambrian. Substantial carbonate burial on (or in) ocean crust could be accompanied by a relative paucity of carbonate in coeval cratonic deposits, similar to the seesaw observations from the Mesozoic–Cenozoic (Fig. 7). Unlike in the Mesozoic and Cenozoic, however, deep ocean Proterozoic $CaCO_3$ burial would have been accomplished through abiotic and/or microbially-mediated precipitation (Grotzinger and James, 2000), transport of shallowly-produced $CaCO_3$ to more prevalently carbonate-saturated slope/abyssal settings (Zeebe and Westbroek, 2003; Higgins et al., 2009; Bergmann et al., 2013), or through extensive carbonate addition to oceanic crust via vein formation. Regardless of the mechanism, if there is a missing Precambrian $CaCO_3$ sink, then it should have a similar mean $\delta^{44}Ca$ value to both preserved Precambrian carbonates and the bulk silicate Earth, in order to satisfy Ca isotope mass balance (Blättler and Higgins, 2017).

4.4. Continental carbonate burial flux across Earth history

Considering total continental $CaCO_3$ mass argues even more strongly for significant carbonate burial on Precambrian oceanic crust (Fig. 8). A carbonate volume time series can be estimated for North America by calculating the carbonate volume of each rock unit in Macrostrat columns, using its average thickness, areal extent, and assigned lithologies. This volume is then converted into moles of $CaCO_3$, which is distributed linearly between the bottom and top age of each unit. Summing over all units results in a time series of carbonate mass burial flux. This time series is scaled up to a global estimate by defining a scale factor needed to match the time series of North American carbonate area (blue in Fig. 2A) with a global time series of carbonate area in the Phanerozoic (binned to geologic epochs, Ronov et al., 1980). Because such scaling factors cannot be determined for the Proterozoic, the minimum (2.0) and maximum (19.8) Epoch scale factors were used to provide bounds on the likely global continental carbonate mass flux in the Proterozoic (shaded blue region in Fig. 8). Global scaling from Macrostrat's North American coverage predicts that Earth's total global continental sedimentary shell contains 5.3×10^{21} moles of $CaCO_3$, which is within 6% of other such estimates (5×10^{21} moles from Berner, 1989), although this estimate also comes from geologic compilations by Ronov.

Unlike relative carbonate abundance, this time series is driven by changes in total sedimentary rock quantity in continental crust (Fig. 2A), which exhibits an order-of-magnitude increase across the Neoproterozoic-Paleozoic transition (Peters and Gaines, 2012; Husson and Peters, 2017; Peters et al., 2022; Walton et al., 2023; Segessenman and Peters, 2023). We compare this time series of absolute carbonate abundance to an estimate of average Phanerozoic volcanic outgassing rate (3.4×10^{18} moles C per Myr. from Coogan and Gillis, 2020). Total carbonate burial rate does not equate to outgassing rate, because outgoing carbon is also buried as organic matter and because carbonate burial must also balance carbonate weathering. Nevertheless, the comparison is useful, and it is notable that the Proterozoic mean is 1.35×10^{17} – 1.33×10^{18} moles of $CaCO_3$ per Myr., equivalent to ×0.04 – 0.39 average Phanerozoic volcanic outgassing.

By contrast, in the Cambrian, preserved carbonate burial flux on the continents reaches ×7.5 Phanerozoic outgassing rates. From this early Paleozoic high, carbonate mass per Myr. declines fitfully (but persistently) to the end of the Paleozoic (Fig. 8). Across the Mesozoic Era, values oscillate, but the time series does not show notable long-term secular trends. Starting in the Cenozoic, values again decline towards the recent. Note that ours is a conservative estimate for the amount of carbonate originally deposited on continental crust because it is based only on the surviving amount.

These secular patterns in surviving continental $CaCO_3$ mass, where the greatest values are observed ~500 million years ago, are not congruent with the expectations of standard rock cycling models (e.g., Gregor, 1970). Instead, it is more likely that changes in surviving continental carbonate mass are controlled predominantly by changes in how much carbonate originally accumulated on continental crust – an interpretation previously suggested for both Phanerozoic carbonates (Walker et al., 2002) and for all Phanerozoic sedimentary rocks (Ronov et al., 1980; Peters and Husson, 2017). In this view, the most striking feature in the history of carbonate abundance in continental crust is a large, relatively abrupt increase in the total mass from the Neoproterozoic to the early Paleozoic. Even if we assume that significant carbonate is buried as disseminated $CaCO_3$ in siliciclastic sediments, this pattern remains. As an extreme example, if 25% of Proterozoic siliciclastic rock volume is $CaCO_3$, then the average Proterozoic burial rate rises to 1.52×10^{18} moles of $CaCO_3$ per Myr., or ×0.18 – 0.45 volcanic outgassing. Thus, the increase cannot be explained fully as a shift from more disseminated carbonate burial in the Proterozoic to more concentrated, pure carbonate burial in the Paleozoic.

If, instead, we assume that CO_2 outgassing did not dramatically increase across this boundary, then the simplest explanation for the observed history of carbonate abundance is an abrupt shift in the locus of carbonate (and all sediment) burial (Fig. 9): from oceanic crust during much of the Proterozoic, where it was continually recycled via subduction and not preserved, to continental crust, where it was sequestered and preserved on longer timescales, right up to the present day.

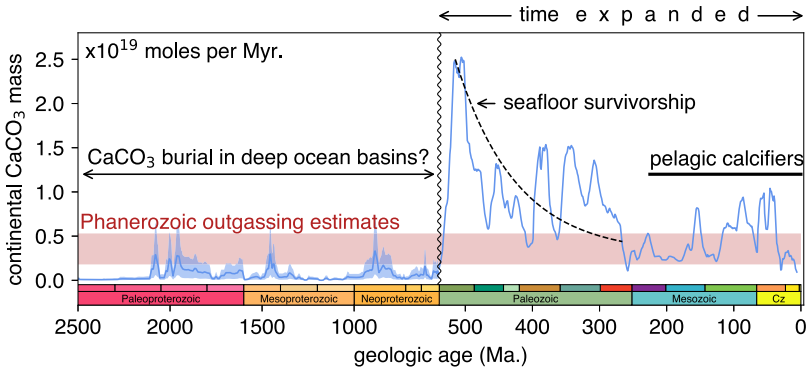

Fig. 8. A record of carbonate mass flux on continental crust is presented (10 Myr running average, in 10^{19} moles $CaCO_3$ per Myr.). Also shown are lower and upper estimates of average Phanerozoic outgassing rates from Coogan and Gillis (2020), and the age range of pelagic calcifiers (Bown et al., 2004). Dashed line is a scaled survivorship curve for Precambrian-aged oceanic crust, assuming the half-life of deep sea floor determined from the modern seafloor (Rowley, 2002). Note that the *x*-axis scale is different between the Precambrian and Phanerozoic portions of the figure.

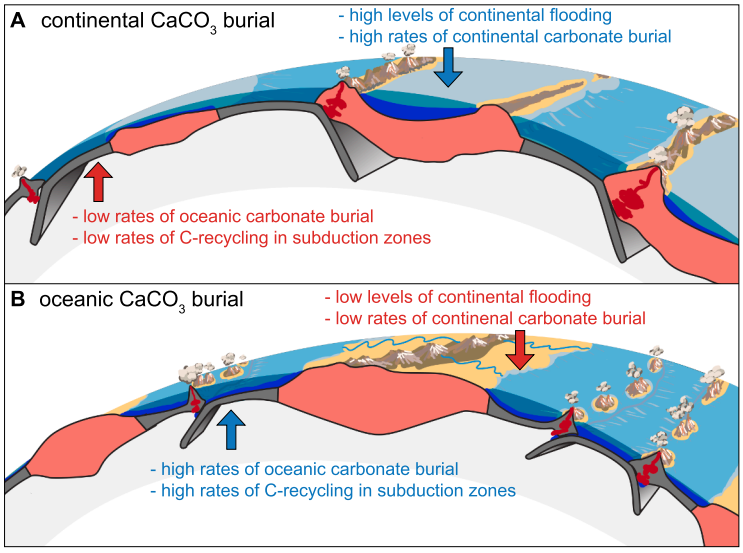

Fig. 9. A schematic cartoon showing contrasting modes of carbonate burial between continental and oceanic crust. (A) High levels of continental flooding enhance carbonate burial (dark blue) and storage on continental crust (pink), leaving little carbonate flux for accumulation on oceanic crust (grey). The resultant decrease in the carbon content of seafloor sediments contributes to lower CO_2 input from arcs. (B) Low levels of continental flooding necessitate a shift in carbonate burial to oceanic crust, which increases the carbon content of sediments entering subduction zones. This state can lead to higher CO_2 input from arcs. The rock record provides evidence for a relatively abrupt shift during the Ediacaran-Cambrian transition from a protracted "B" state in the Precambrian to an "A" state in the Paleozoic. Illustrations courtesy of Evgeny Mazko.

4.5. Implications of Precambrian deep sea carbonate burial and a Paleozoic shift to continental carbon sequestration

An implication of a shift in the primary locus of carbonate burial from the deep sea floor in the Precambrian to continental shelves in the Paleozoic is that Proterozoic-aged ocean crust was laden with Proterozoic-aged carbonate, with a much smaller continental carbonate reservoir. Such a state could have led to reduced Proterozoic carbonate weathering rates (and associated carbonate burial rates) when compared to the Phanerozoic. It is also possible that deep-sea carbonate ended up in accretionary prisms and subduction zone complexes, making it available for weathering and rapid recycling in active margins (Fig. 9). After the Proterozoic-Paleozoic transition, when most carbonate burial shifted up onto continental crust, reflected in a large expansion in the area of shallow continental seas (Tasistro-Hart and Macdonald, 2023), all newly formed Paleozoic seafloor would have necessarily been deprived of carbonate sediment. Throughout the Paleozoic, as carbonate-bearing, Precambrian-aged ocean crust was consumed at convergent margins, it was replaced with Paleozoic-aged seafloor with little or no carbonate, resulting in a Paleozoic deep ocean floor with progressively less and less carbonate sediment.

A declining quantity of seafloor carbonate available for volatilization during subduction (Fig. 8 and 9) predicts a first-order decline in subduction fluxes of CO_2. Although the estimated decarbonation efficiency of modern subducted sediments is highly variable (18 – 70% from Johnston et al., 2011), a major component of CO_2 emissions by arc volcanoes derives from subducted and recycled carbon (Plank and Manning, 2019; Arzilli et al., 2023). In particular, compilations of $\delta^{13}C$ values of arc gases suggest that carbonates are a dominant source for this recycled carbon (average of 70%, Kagoshima et al., 2015). Thus, the Paleozoic likely experienced initially high, and then declining, carbon inputs from subduction zones, as carbonate-rich Precambrian seafloor was progressively destroyed and replaced with carbonate-poor Paleozoic seafloor. This prediction is consistent with isotopic reconstructions of the Cambrian carbon cycle, which suggest that carbon input fluxes were ×4 – 16 modern levels (Maloof et al., 2010), and with Phanerozoic Earth

system models (Berner, 2006; Bergman et al., 2004) and proxies (Royer, 2014) that contend atmospheric CO_2 levels decreased by a factor of 5 – 6 across the Paleozoic Era.

The notion that much of the Paleozoic-aged carbonate that is still sequestered on the continents today was derived from the recycling of carbonate-laden, Proterozoic-aged seafloor is plausible, given our estimate for the amount of carbon in Paleozoic continental carbonate (2.97×10^{21} moles), the area of modern oceanic crust (2.95×10^{8} km^2, Seton et al., 2012), and modern rates of seafloor subduction (2.96 km^2 per yr., Rowley, 2002). If surviving Paleozoic carbonate were evenly distributed over this same area of seafloor and subducted at the modern rate, then the early Paleozoic peak in carbon input contributed by subducting carbonates (assuming complete recycling) would be 2.98×10^{19} moles per Myr., or ×8.8 the estimated average Phanerozoic outgassing rate. Note that because the geographic distribution of carbon-bearing sediments on Proterozoic sea floor was likely heterogeneous, just as it is today, shifts in the location of subduction zones during the Precambrian and Paleozoic could have resulted in relatively abrupt shifts in the amount and composition of carbon-bearing sediments entering subduction zones. This type of shift has been invoked to help explain climate trends in the Cenozoic, with the cessation of subduction of carbon-rich Tethyan ocean crust in the Early Eocene (combined with a shift in subduction to carbon-poor Pacific seafloor) contributing to a decline in CO_2 outgassing and Cenozoic cooling (Kent and Muttoni, 2008).

When the potential timing of subduction of Precambrian-aged sea floor during the Paleozoic is considered, another implication for the Earth system is raised. Modern rates of seafloor spreading and subduction (Rowley, 2002) would imply that all Proterozoic-aged sea floor was destroyed by the latest Paleozoic (dashed line in Fig. 8). Thus, by the time all of the carbonate-laden Precambrian sea floor was subducted and recycled near the end of the Paleozoic, the entire deep ocean may have been left nearly devoid of carbonate sediment – a short-lived state that may have been unique in the Phanerozoic, and possibly most of Earth history (Figs. 3, 8 and 9). A deep ocean with little carbonate sediment is inherently more weakly buffered against acidification from CO_2 injections (Zeebe and Westbroek, 2003), particularly during sea level falls which remove continental shelf carbonates from contact with seawater. The possibility that the global ocean was unbuffered in the Paleozoic, when compared to the Mesozoic and Cenozoic, has been raised previously (e.g., Payne et al., 2007). Our results suggest that the *terminal* Paleozoic was uniquely unbuffered compared to the rest of the Phanerozoic. This unusual state could have contributed to the notable severity and selectivity of the end-Permian mass extinction, during which taxa vulnerable to hypercapnia and ocean acidification were preferentially eliminated (Knoll et al., 2007; Payne et al., 2007).

5. Conclusion

The age and quantity of carbonate sediments in continental crust suggests that the principal burial locus of carbonate (and all sediments) has oscillated over geologic time. Specifically, there is evidence to suggest that the Paleozoic may have been unique in most of Earth history, with the continents shifting rather abruptly in the early Paleozoic to accommodate most, and possibly all, of the global carbonate (and organic carbon) burial flux (Fig. 9). Capturing most of the global carbon burial flux on continental shelves likely left oceanic crust formed in the Paleozoic depleted in carbonate. Progressive subduction of carbonate-rich Precambrian sea floor during the Paleozoic, and its replacement with carbonate-depleted Paleozoic-aged sea floor, could have contributed to a first-order decrease in volcanic CO_2 input fluxes during the Paleozoic. Depletion of carbonate sediment in the deep sea would have also decreased the buffering capacity of the ocean and made the latest Paleozoic surface environment more sensitive to CO_2 injections, particularly when operating in concert with sea level falls that remove carbonate shelf sediments from contact with seawater. This late Paleozoic state, possibly unique in at least the past billion years, may have contributed to the overall sensitivity of the Earth system to end-Permian CO_2 perturbations. The evolution of pelagic calcifying organisms early in the Mesozoic, and a decrease in tropical continental shelf area due in part to the northward drift of the continents and overall reduction in continental flooding, likely repositioned oceanic crust as an important locus for carbonate burial.

CRediT authorship contribution statement

Jon M. Husson: Writing – original draft, Visualization, Methodology, Formal analysis, Conceptualization; **Shanan E. Peters:** Writing – review & editing, Data curation, Conceptualization.

Data availability

All Macrostrat column data are made publicly available via the Macrostrat API (Peters et al., 2018). All time series of sediment area, carbonate area, fraction carbonate and carbonate mass presented here are also included in a Supplementary Excel file.

Declaration of competing interest

The authors declare that they have no known competing financial interests or personal relationships that could have appeared to influence the work reported in this paper.

Acknowledgements

Macrostrat was developed primarily with the support of NSF grants EAR-1948843 and ICER-1928323 to SEP. Ongoing development is in part supported by NSF CSSI-2311091 and NSF OSE-2324579. We thank Lee Kump for comments on an earlier draft of this manuscript, and Evgeny Mazko for drafting the block diagrams shown in Fig. 9. We thank John Higgins, Dietmar Müller and an anonymous reviewer for constructive reviews that improved the manuscript, and Tristan Horner for editorial review.

Supplementary material

Supplementary material associated with this article can be found in the online version at 10.1016/j.epsl.2025.119810

References

Arzilli, F., Burton, M., La Spina, G., Macpherson, C.G., van Keken, P.E., McCann, J., 2023. Decarbonation of subducting carbonate-bearing sediments and basalts of altered oceanic crust: insights into recycling of CO_2 through volcanic arcs. Earth Planet. Sci. Lett. 602, 117945.
Asch, K., 2003. The 1:5 million international geological map of Europe and adjacent areas. Map. Schweizerbart Science Publishers, Stuttgart, Germany.
Bergman, N.M., Lenton, T.M., Watson, A.J., 2004. COPSE: A new model of biogeochemical cycling over Phanerozoic time. Am. J. Sci. 304, 397–437.
Bergmann, K.D., Grotzinger, J.P., Fischer, W.W., 2013. Biological influences on seafloor carbonate precipitation. Palaios 28, 99–115.
Berner, R.A., 1989. Biogeochemical cycles of carbon and sulfur and their effect on atmospheric oxygen over Phanerozoic time. Glob. Planet. Change 1, 97–122.
Berner, R.A., 2006. GEOCARBSULF: A combined model for Phanerozoic atmospheric O_2 and CO_2. Geochim. Cosmochim. Acta 70, 5653–5664.
Berry, J.P., Wilkinson, B.H., 1994. Paleoclimatic and tectonic control on the accumulation of North American cratonic sediment. Geol. Soc. Am. Bull. 106, 855–865.
Blatt, H., Jones, R.L., 1975. Proportions of exposed igneous, metamorphic, and sedimentary rocks. Geol. Soc. Am. Bull. 86, 1085–1088.
Blättler, C.L., Higgins, J.A., 2017. Testing Urey's carbonate–silicate cycle using the calcium isotopic composition of sedimentary carbonates. Earth Planet. Sci. Lett. 479, 241–251.
Boss, S.K., Wilkinson, B.H., 1991. Planktogenic/eustatic control on cratonic/oceanic carbonate accumulation. J. Geol. 99, 497–513.
Bown, P.R., Lees, J.A., Young, J.R., 2004. Calcareous nannoplankton evolution and diversity through time. Springer Berlin Heidelberg, Berlin, Heidelberg. 481–508
Broecker, W.S., Peng, T.H., 1987. The role of $CaCO_3$ compensation in the glacial to interglacial atmospheric CO_2 change. Glob. Biogeochem. Cycles 1, 15–29.

Buitenhuis, E.T., Li, W.K.W., Vaulot, D., Lomas, M.W., Landry, M.R., Partensky, F., Karl, D.M., Ulloa, O., Campbell, L., Jacquet, S., Lantoine, F., Chavez, F., Macias, D., Gosselin, M., McManus, G.B., 2012. Picophytoplankton biomass distribution in the global ocean. Earth Syst. Sci. Data 4, 37–46.
Coffey, J., Flannery, D., Walter, M., George, S., 2013. Sedimentology, stratigraphy and geochemistry of a stromatolite biofacies in the 2.72 Ga Tumbiana Formation, Fortescue Group, Western Australia. Precambrian Res. 236, 282–296.
Coogan, L., Gillis, K., 2020. The average Phanerozoic CO_2 degassing flux estimated from the O-isotopic composition of seawater. Earth Planet. Sci. Lett. 536, 116151.
Dittrich, M., Kurz, P., Wehrli, B., 2004. The role of autotrophic picocyanobacteria in calcite precipitation in an oligotrophic lake. Geomicrobiol. J. 21, 45–53.
Edmond, J.M., Huh, Y., 2003. Non-steady state carbonate recycling and implications for the evolution of atmospheric pCO_2. Earth Planet. Sci. Lett. 216, 125–139.
Fraass, A.J., Kelly, D.C., Peters, S.E., 2015. Macroevolutionary history of the planktic foraminifera. Annu. Rev. Earth Planet. Sci. 43, 139–166.
Furnes, H., De Wit, M., Dilek, Y., 2014. Four billion years of ophiolites reveal secular trends in oceanic crust formation. Geosci. Front. 5, 571–603.
Furnes, H., Dilek, Y.d., De Wit, M., 2015. Precambrian greenstone sequences represent different ophiolite types. Gondwana Res. 27, 649–685.
Gaillardet, J., Calmels, D., Romero-Mujalli, G., Zakharova, E., Hartmann, J., 2019. Global climate control on carbonate weathering intensity. Chem. Geol. 527, 118762.
Gaillardet, J., Dupré, B., Louvat, P., Allegre, C., 1999. Global silicate weathering and CO_2 consumption rates deduced from the chemistry of large rivers. Chem. Geol. 159, 3–30.
Gregor, B., 1970. Denudation of the continents. Nature 228, 273–275.
Grotzinger, J.P., James, N.P., 2000. Precambrian carbonates: evolution of understanding. In: Grotzinger, J.P., James, N.P. (Eds.), Carbonate Sedimentation and Diagenesis in the Evolving Precambrian World. Special Publications of SEPM.
Harrison, J.C., St-Onge, M.R., Petrov, O.V., Strelnikov, S.I., Lopatin, B.G., Wilson, F.H., Tella, S., Paul, D., Lynds, T., Shokalsky, S.P., Hults, C.K., Bergman, S., Jepsen, H.F., Solli, A., 2011. Geological map of the Arctic. Map. Natural Resources Canada. 2159A.
Hayes, J.M., Waldbauer, J.R., 2006. The carbon cycle and associated redox processes through time. Philos. Trans. R. Soc. B: Biol. Sci. 361, 931–950.
Higgins, J., Fischer, W., Schrag, D., 2009. Oxygenation of the ocean and sediments: consequences for the seafloor carbonate factory. Earth Planet. Sci. Lett. 284, 25–33.
Horton, J.D., San Juan, C.A., Stoeser, D.B., 2017. The state geologic map compilation (SGMC) geodatabase of the conterminous United States. Report. Reston, VA, United States, Geologic Survey.
Husson, J.M., Peters, S.E., 2017. Atmospheric oxygenation driven by unsteady growth of the continental sedimentary reservoir. Earth Planet. Sci. Lett. 460, 68–75.
Husson, J.M., Peters, S.E., 2018. Nature of the sedimentary rock record and its implications for Earth system evolution. Emerg. Top. Life Sci. 2, 125–136.
Johnston, F.K., Turchyn, A.V., Edmonds, M., 2011. Decarbonation efficiency in subduction zones: implications for warm Cretaceous climates. Earth Planet. Sci. Lett. 303, 143–152.
Kagoshima, T., Sano, Y., Takahata, N., Maruoka, T., Fischer, T.P., Hattori, K., 2015. Sulphur geodynamic cycle. Sci. Rep. 5, 8330.
Kalderon-Asael, B., Wang, J., Planavsky, N.J., Oehlert, A.M., Vitek, B.E., Reid, R.P., Tarhan, L.G., 2025. Evaluation of early diagenetic signatures of lithium and stable strontium isotopes in shallow marine carbonate sediments. Chem. Geol. 676, 122590.
Kent, D.V., Muttoni, G., 2008. Equatorial convergence of India and early Cenozoic climate trends. Proc. Natl. Acad. Sci. 105, 16065–16070.
Knoll, A.H., Bambach, R.K., Payne, J.L., Pruss, S., Fischer, W.W., 2007. Paleophysiology and end-Permian mass extinction. Earth Planet. Sci. Lett. 256, 295–313.
Kump, L.R., Arthur, M.A., 1997. Global chemical erosion during the Cenozoic: weatherability balances the budgets. In: Tectonic Uplift and Climate Change. Springer, pp. 399–426.
Lees, A., 1975. Possible influence of salinity and temperature on modern shelf carbonate sedimentation. Mar. Geol. 19, 159–198.
Maloof, A.C., Ramezani, J., Bowring, S.A., Fike, D.A., Porter, S.M., Mazouad, M., 2010. Constraints on early Cambrian carbon cycling from the duration of the Nemakit–Daldynian–Tommotian boundary δ^{13}c shift, morocco. Geology 38, 623–626.
Merdith, A.S., Collins, A.S., Williams, S.E., Pisarevsky, S., Foden, J.D., Archibald, D.B., Blades, M.L., Alessio, B.L., Armistead, S., Plavsa, D., et al., 2017. A full-plate global reconstruction of the Neoproterozoic. Gondwana Res. 50, 84–134.
Milliman, J., Droxler, A., 1996. Neritic and pelagic carbonate sedimentation in the marine environment: ignorance is not bliss. Geol. Rundsch. 85, 496–504.
Morse, J., 2005. Formation and diagenesis of carbonate sediments. In: Mackenzie, F.T. (Ed.), Sediments, Diagenesis, and Sedimentary Rocks: Treatise on Geochemistry. Elsevier. Vol. 7.
Müller, R.D., Cannon, J., Qin, X., Watson, R.J., Gurnis, M., Williams, S., Pfaffelmoser, T., Seton, M., Russell, S.H., Zahirovic, S., 2018. GPlates: building a virtual Earth through deep time. Geochem. Geophys. Geosyst. 19, 2243–2261.
Opdyke, B.N., Wilkinson, B.H., 1988. Surface area control of shallow cratonic to deep marine carbonate accumulation. Paleoceanography 3, 685–703.
Payne, J.L., Lehrmann, D.J., Follett, D., Seibel, M., Kump, L.R., Riccardi, A., Altiner, D., Sano, H., Wei, J., 2007. Erosional truncation of uppermost Permian shallow-marine carbonates and implications for Permian-Triassic boundary events. Geol. Soc. Am. Bull. 119, 771–784.
Peters, S.E., Gaines, R.R., 2012. Formation of the "Great Unconformity" as a trigger for the Cambrian explosion. Nature 484, 363–366.
Peters, S.E., Husson, J.M., 2017. Sediment cycling on continental and oceanic crust. Geology 45, 323 – 326.
Peters, S.E., Husson, J.M., Czaplewski, J., 2018. Macrostrat: a platform for geological data integration and deep-time Earth crust research. Geochem. Geophys. Geosyst. 19, 1393–1409.
Peters, S.E., Kelly, D.C., Fraass, A.J., 2013. Oceanographic controls on the diversity and extinction of planktonic foraminifera. Nature 493, 398–401.
Peters, S.E., Quinn, D.P., Husson, J.M., Gaines, R.R., 2022. Macrostratigraphy: insights into cyclic and secular evolution of the Earth-life system. Annu. Rev. Earth Planet. Sci. 50, 419–449.
Plank, T., Manning, C.E., 2019. Subducting carbon. Nature 574, 343–352.
Raymond, O., Liu, S., Gallagher, R., Highet, L., Zhang, W., 2012. Surface geology of Australia, 1:1 000 000 scale, 2012 edition [digital dataset]. Technical Report, Geoscience Australia, Commonwealth of Australia, Canberra.
Ridgwell, A., 2005. A mid Mesozoic revolution in the regulation of ocean chemistry. Mar. Geol. 217, 339–357.
Ronov, A., Khain, V., Balukhovsky, A., Seslavinsky, K., 1980. Quantitative analysis of Phanerozoic sedimentation. Sediment. Geol. 25, 311–325.
Rowley, D.B., 2002. Rate of plate creation and destruction: 180 Ma to present. Geol. Soc. Am. Bull. 114, 927–933.
Royer, D., 2014. Atmospheric CO_2 and O_2 during the Phanerozoic: tools, patterns, and impacts. In: Holland, H.D., Turekian, K.K. (Eds.), Treatise on Geochemistry (Second Edition). Elsevier, Oxford, pp. 251 – 267.
Segessenman, D.C., Peters, S.E., 2023. Macrostratigraphy of the Ediacaran system in North America. In: Whitmeyer, S., Williams, M., Kellett, D., Tikoff, B. (Eds.), Laurentia: Turning Points in the Evolution of a Continent. Geological Society of America Memoir 220, pp. 399–424.
Seton, M., Gaina, C., Müller, R., Heine, C., 2009. Mid-Cretaceous seafloor spreading pulse: fact or fiction? Geology 37, 687–690.
Seton, M., Müller, R.D., Zahirovic, S., Gaina, C., Torsvik, T., Shephard, G., Talsma, A., Gurnis, M., Turner, M., Maus, S., et al., 2012. Global continental and ocean basin reconstructions since 200 Ma. Earth Sci. Rev. 113, 212–270.
Swanson-Hysell, N.L., 2021. The Precambrian paleogeography of Laurentia. In: Ancient Supercontinents and the Paleogeography of the Earth. Elsevier.
Tasistro-Hart, A.R., Macdonald, F.A., 2023. Phanerozoic flooding of North America and the Great Unconformity. Proc. Natl. Acad. Sci. 120, e2309084120.
Thompson, J.B., Schultze-Lam, S., Beveridge, T.J., Des Marais, D.J., 1997. Whiting events: biogenic origin due to the photosynthetic activity of cyanobacterial picoplankton. Limnol. Oceanogr. 42, 133–141.
Torsvik, T.H., Cocks, L.R.M., 2017. Earth history and palaeogeography. Cambridge University Press.
Walker, J.C., Hays, P., Kasting, J.F., 1981. A negative feedback mechanism for the long-term stabilization of Earth's surface temperature. J. Geophys. Res.: Oceans 86, 9776–9782.
Walker, L.J., Wilkinson, B.H., Ivany, L.C., 2002. Continental drift and Phanerozoic carbonate accumulation in shallow-shelf and deep-marine settings. J. Geol. 110, 75–87.
Walton, C.R., Hao, J., Huang, F., Jenner, F.E., Williams, H., Zerkle, A.L., Lipp, A., Hazen, R.M., Peters, S.E., Shorttle, O., 2023. Evolution of the crustal phosphorus reservoir. Sci. Adv. 9, eade6923.
Wang, J., Tarhan, L.G., Jacobson, A.D., Oehlert, A.M., Planavsky, N.J., 2023. The evolution of the marine carbonate factory. Nature 615, 265–269.
Wilkinson, B.H., Consuegra, N.P., 2024. On the crumpling and repaving of the North American continent. Geol. Soc. Am. Bull. 136, 2051–2062.
Wilkinson, B.H., Walker, J.C., 1989. Phanerozoic cycling of sedimentary carbonate. Am. J. Sci. 289, 525–548.
Zeebe, R.E., Westbroek, P., 2003. A simple model for the $CaCO_3$ saturation state of the ocean: the "Strangelove," the "Neritan," and the "Cretan" ocean. Geochem. Geophys. Geosyst. 4.